

# **SLATS Radiometric Correction: a semi-automated, multi-stage process for the standardisation of temporal and spatial radiometric differences.**

Lisa J. Collett, Bruce M. Goulevitch and Tim J. Danaher

Climate Impacts and Grazing Systems  
Resource Sciences Centre  
Queensland Department of Natural Resources  
80 Meiers Road Indooroopilly, 4068  
lisa.collett@dnr.qld.gov.au  
URL: <http://www.dnr.qld.gov.au/slats/>

## **Abstract**

*The Statewide Landcover and Trees Study (SLATS) is mapping change in woody vegetation cover for the periods 1988-91, 1991-95 and 1995-97 and woody vegetation density as of 1991. This analysis is being carried out for 88 Landsat scenes covering the entire state of Queensland. The comparison of imagery from different dates and mosaicing of products from different Landsat paths requires that the imagery is radiometrically corrected.*

*The spectral signatures that are represented in raw satellite data are made up of several influences including the intrinsic features of the ground object, sensor characteristics, environmental conditions, date of acquisition, atmospheric absorption and scattering, and sun-target-satellite geometry (Muller, 1993). SLATS has implemented a series of rapid, easy to apply, correction processes to minimise the effect of these influences on image interpretation and classification. The methods are presented, and include i) conversion to top-of -the-atmosphere-reflectance units, ii) relative scene to scene temporal registration, and iii) relative correction between adjacent scenes.*

*Field results and visual interpretation of Landsat scenes, thematic vegetation density and change products show that the radiometric correction methods markedly reduce edge effects and improve accuracy in the final products.*

## **Introduction**

The Statewide Landcover and Trees Study (SLATS) (Danaher *et al.*, 1998) was commenced in 1995 by the Queensland Department of Natural Resources to provide objective baseline information on woody vegetation and landcover, and to quantify the change in woody vegetation due to land clearing, regrowth and woodland thickening over time. The information is in demand by numerous stakeholders for policy planning, assessment of natural resource and greenhouse gas inventories, and other associated research.

Landsat TM scenes covering the entire state of Queensland have been acquired for the periods 1988, 1991, 1995 and 1997. Complete coverage of Queensland requires 88 Landsat TM scenes distributed over 12 Landsat paths. SLATS has developed a satellite image and field measurement based methodology which relies heavily on quantitative spatial and temporal analysis of these data. Thus in the developmental stages of the project one of the significant challenges was to develop practical methods of preprocessing these data to standardise the radiometric differences which are evident between adjacent scenes and multi-date imagery. This paper presents the radiometric correction techniques adopted by SLATS to address these issues.

Correction of spatial and temporal radiometric differences are critical for the SLATS baseline mapping methods. These methods use field measurements to calibrate an empirical relationship between image response and woody vegetation cover on a scene by scene basis. Although the relationship is computed for an individual TM scene, field sites from adjacent scenes are used in

the calibration. Differences in the acquisition environments for adjacent scenes result in edge effects which make it impossible to perform these multi-scene calibrations on radiometrically uncorrected data. Correcting for these spatial differences also increases the quality of the final mosaiced products, including false colour Landsat TM series, landcover series and woody vegetation change for Queensland (Walls *et al.*, 1998). Users of these end products receive seamless data sets which enhance the user-friendliness of the final products.

A relative temporal radiometric registration between 1988, 1991 and 1995 data is also required so that all three dates of imagery can be used to normalise the vegetation effects over time, stabilising the relationship between cover and image response. These methods developed for mapping woody vegetation cover are detailed by Kuhnell *et al.* (1998).

The SLATS requirements for a radiometric correction are very much dictated by operational practicalities. In dealing with such large databases all SLATS processing methods have, where possible, been automated. In this way SLATS has tried to reduce the differences resulting from analyst interpretation. With a team of twelve remote sensing analysts employed by the project, a level of automation of processing stages was considered vital.

## Review

A common radiometric benchmark is needed for quantitative analysis of remotely sensed images over space and time. The spectral information recorded in raw satellite data is made up of several influences including the intrinsic features of the ground object, sensor characteristics, environmental conditions, atmospheric absorption and scattering, and sun-target-satellite geometry (Muller, 1993). These combine to produce significant band-dependent radiometric differences, confounding the interpretation of both temporal and spatial data sets, particularly when added to the dynamic on-ground physical variations affecting spectral response e.g. ephemeral greening after rainfall, gross cover changes.

SLATS has benefited from the considerable research, which has been conducted over the last twenty years, investigating radiometric influences on ground response. Two approaches to correcting for confounding radiometric variations in multi-date imagery emerge in the literature. The first aims to individually account for some or all radiometric effects on surface response by converting digital data to physical units of radiance, using sensor calibration coefficients - detailed in Holm *et al.* (1989); top-of-atmosphere (TOA) reflectance correcting for illumination variations; and ground reflectance correcting for atmospheric effects (e.g. Moran *et al.*, 1990; Moran *et al.*, 1992; Muller, 1993; and Vermote *et al.*, 1994). The second aims to empirically correct for relative radiometric differences existing between multiple data sets through radiometric registration i.e. registering one data set to another so it appears as if both were acquired under the same set of conditions (e.g. Hall *et al.*, 1991; Muller, 1993).

One of the biggest problems to overcome in the first approach is to adequately correct for atmospheric effects. Continued efforts to measure and model radiation transfer and atmospheric dynamics have resulted in a number of radiative transfer models (RTMs) which provide reasonable estimates of atmospheric attenuation and scattering (Herman and Browning, 1975; Vanouplines, 1986; Vermote *et al.*, 1994). The more complex of these models attempt to make allowances for non-Lambertian reflectance e.g. the 6S code developed by Vermote *et al.* (1994). There is a trade-off here between the need for accurate correction and the realistic requirements for operational implementation over large areas and many acquisition dates. Application of RTMs depend on knowledge of standard meteorological variables at the time of acquisition or on simulation of the vertical profile of the atmosphere under a variety of conditions (Vermote *et al.*, 1994).

Because of these limitations other studies have attempted to estimate the atmospheric component by calibrating pixel values with surface reflectances measured on the ground at the time of acquisition (e.g. Holm *et al.*, 1989) (logistically impractical for the SLATS project) or by deriving it directly from the image as in the Dark Object Subtraction (Chavez, 1989), Reflection Intersection Method (Crippen, 1987), and Covariance Matrix Method (Switzer *et al.*, 1981). These methods are conceptually simple but rely on the existence of certain scene elements (e.g. the presence of a zero reflectance surface such as a deep water body), are analyst dependent and difficult to be automate and apply over 88 scenes.

The absolute correction approach was found to be impractical for application across 88 multi-temporal data sets. Historical meteorological data does exist for Queensland but coverage is incomplete, and almost never available at the required resolution. However the correction for variation in solar zenith and incident solar radiation (earth-sun distance) is applied and detailed in the next section.

SLATS has adopted a relative radiometric registration method which aims to empirically correct multi-date and spatial radiometric variations. The radiometric registration techniques mentioned earlier assume that in any given scene there are a number of target pixels that have relatively invariant spectral properties. Schott *et al.* (1988) used pseudoinvariant targets, largely urban features to form the basis of a multi-date histogram normalisation registration. The method provided an adequate level of registration although for SLATS purposes is impractical as a lot of western Queensland scenes do not contain any urban pixels and the potential non-Lambertian nature of urban reflectance may introduce radiometric bias into target selection. Hall *et al.* (1991) successfully tested the assumption that some of the pixels located in the non-vegetated extreme of the Kauth-Thomas (K-T) distribution of greenness and brightness will be relatively spectrally invariant. Although this assumption has been accepted by others (Muller, 1993) the radiometric control sets used by Hall *et al.* weren't necessarily the same on each date i.e. they assumed that the K-T distribution always corresponded to the same dynamic range of brightness on each image - relative differences were only a result of atmospheric/sensor effects which shrink and rotate the K-T distribution in a linear way. This assumption does not allow for excessive cloud or heavy rainfall which can affect the shape and behaviour of the K-T extremes. The SLATS method for registering multi-date data uses bright and dark targets but differs from Hall *et al.* in that targets are from the same location in each date.

The empirical methods outlined above focus very much on registration of spatially concurrent data sets and assume minimal within-scene variation in radiometric effects. Early SLATS experimentation with adjacent east-west TM scene pairs showed consistently that the western side of a scene was brighter than the eastern side. No further investigation of the cause of these effects was conducted. Our findings, however, are consistent with those documented in the literature for other sensors with steeper off-nadir look angles and wider scan angles e.g. airborne scanners (Royer *et al.*, 1985; Whitlock *et al.*, 1994) and SPOT High-Resolution-Visible (HRV) (Moran *et al.*, 1990; Muller, 1993). This effect has been attributed to the combined influences of ground target structure, sensor wavelength, and the sun-target-satellite geometry (Royer *et al.*, 1985; Moran *et al.*, 1990; Muller, 1993; and Whitlock *et al.*, 1994) and documented to be asymmetric about the nadir position, and non-linear for cases of large viewing angles (greater than 40°) (Royer *et al.*, 1985; Paltridge and Mitchell, 1990; Whitlock *et al.*, 1994). SLATS theorises that our within-scene east-west differences are caused by the additive effects of anisotropic reflectance and relative atmospheric offsets between adjacent scenes. An empirical correction based on statistics from path overlap areas was developed to minimise these effects.

The SLATS methods detailed in this paper include:-

- conversion to TOA units to correct for varying illumination conditions;
- registration of temporal sets to correct for relative atmospheric effects between spatially concurrent scenes; and
- spatial registration to correct for the combined influences of atmospheric and anisotropic effects acting within-scene and between spatially adjacent scenes.

## **Conversion to Top of Atmosphere Reflectance**

This stage involves automatic conversion of Landsat TM digital numbers (DN) - as supplied by the Australian Centre for Remote Sensing (ACRES) - to "reflectance like units". These are not strictly TOA reflectance units due to the sensor calibration difficulties outlined below.

The conversion is achieved using in house developed FORTRAN code (TM\_REFLECT) which uses information derived from the image header file as inputs. This correction aims to minimise variation due to varying solar zenith angles and incident solar radiation, which are caused by variation in scene dates, overpass time and scene latitude.

Firstly DN values need to be converted to radiance values (L) using the following formula:-

$$L_{\lambda} \text{ (radiance)} = \alpha_{\lambda} \text{ DN} + \beta_{\lambda} W \text{ m}^{-2} \text{ sr}^{-1} \mu\text{m}$$

There is considerable uncertainty about which gain and offset values ( $\alpha_{\lambda}$  &  $\beta_{\lambda}$ ) should be used to convert to radiance. Several possibilities exist:-

- a pre-launch calibration could be used but degradation of the TM sensor is a well documented problem (Slater, 1987);
- in-flight calibration over desert sites (Slater, 1987) could be used. The problem here is that these coefficients are now old. In addition, ACRES level 5 corrected imagery needs to have some processing reversed before these coefficients can be effectively applied; and
- using the TM instruments internal calibration system. This allows for degradation of the sensor but not other parts of the system. The internal calibration method is routinely applied in producing ACRES Level 5 corrected products and is known as the CAL 2 option. It was found that the imagery purchased was calibrated using two differing sets of reference detectors. The 1988 and most 1991 data were processed with one set of values and later 1991 and 1995 imagery with another. Some 1991 data processed with both coefficients were compared in overlap areas and very few differences between the DN values were detected. We are confident that subsequent radiometric correction processes further minimise these differences.

Initially Slater (1987) in-flight calibrations were used to calculate the radiance values. While the use of these coefficients is not ideal - because of changes in ACRES low-level processing - we considered that processing consistency was a priority. Most of the SLATS image processing involves comparisons of TM data over time and space therefore relative registration of data sets is more important than absolute correction. Hence, we continue to use the same calibration values but also have the ability to transform the data if required.

Once radiance values are calculated the reflectance ( $\rho$ ) is then calculated for each band as in Vermote *et al.* (1994):-

$$\rho_{\lambda} = \frac{\pi d^2 L_{\lambda}}{E_{0\lambda} \cos \theta_s}$$

where  $d$  = earth sun distance correction

$L_{\lambda}$  = radiance as a function of bandwidth

$E_{0\lambda}$  = exoatmospheric irradiance

$\theta_s$  = solar zenith angle

The correction is applied on a pixel by pixel basis for each scene. It uses the scene centre position, overpass time and acquisition date derived from the scene header. Subroutines from the S6 code (Vermote *et al.*, 1994) were used to calculate solar zenith angle and the earth sun distance factor. The output reflectance values are scaled to an 8 bit data range.

## Temporal Radiometric Registration

The temporal radiometric registration is applied to spatially concurrent 1988, 1991, and 1995 data sets. This method locates relatively invariant pixels which represent bright and dark targets that are characterised by low 'greenness' on all three dates of imagery. It is assumed that whilst some between scene variation can be expected for individual target pixels, the set of reflectance means for bright and dark target clusters is expected to be stable over time and can therefore be used to derive the transformation parameters (Hall *et al.*, 1991; Muller, 1993) . A series of scripts have been developed to assist the operator in creating the bright and dark target masks, calculate the linear transformation coefficients, and register all scenes to a selected reference image.

## Selection of Bright and Dark Targets

The first script reduces the data in three dates of imagery (18 bands in total) to a four layer composite raster containing information about the greenness and brightness variations across the three dates. Each of the four layers is a composite of pixels from three dates of imagery derived as follows:

1. Maximum NDVI across 1988,1991 and 1995 dates - NDVI is scaled to an 8 bit range.
2. Minimum Brightness across 1988,1991 and 1995 dates where Brightness has been defined as the average of TM bands 2,3,4 and 5;
3. Maximum Brightness across 1988,1991 and 1995 dates; and
4. Coefficient of Variation (CV) in Brightness across 1988,1991 and 1995 where the CV is used as a measure of Brightness variation relative to the mean across three dates where for each set of three spatially concurrent pixels the CV is calculated as:-

$$CV = \sigma / \mu \text{ (88 Brightness, 91 Brightness, 95 Brightness).}$$

Note: we have used the CV to represent Brightness variation for each set of three pixels in the multi-date data sets. In this case the CV is not used as a statistical descriptor as the sample size for each calculation is too small to be statistically valid. However the set of CVs for a whole scene can be statistically analysed because they are generally continuous and normally distributed. This is detailed later.

Determining appropriate thresholds for the selection of bright and dark targets is an iterative process. In the first iteration bright and dark target masks are created by defining thresholds for the NDVI and Brightness composites (layers 1-3) with no initial limits imposed on the CV layer. The resulting two output masks from the first iteration contain CV values for bright and dark targets respectively. In the second iteration thresholds are defined for the bright and dark target CV histograms to omit outlying pixels in the masks which vary from the mean CV. Thresholding of these composite layers to create the final two bright and dark target masks is summarised in Figure 1.

A single greenness threshold is used in the selection of both bright and dark targets. By using the composite of maximum NDVI for three dates (layer 1), only targets that have low greenness on all dates (even on the greenest of scenes) are selected. An NDVI threshold of 0 is used as the default upper limit. For some scenes, however, it has been necessary to increase this threshold slightly to select more targets. This is considered an extreme measure as experience has shown that varying the NDVI threshold seems to have the greatest influence on the final registration parameters.

The bright and dark target mask are created by thresholding the Minimum Brightness (layer 2) and Maximum Brightness composite (layer 3) histograms respectively. The pixels in the right hand tail of the Minimum Brightness frequency histogram represent the pixels which could be considered bright targets on all three dates. The threshold,  $T_b$ , is defined to select only the brightest 0.01% of the frequency histogram. This approximates about 4000 pixels from the whole Minimum Brightness Composite. The threshold,  $T_d$ , for the Maximum Brightness is similarly defined to locate dark targets in the left hand tail of the histogram. Constraining both 'greenness' and Brightness reduces the targets quite significantly to numbers in the order of 300-400 invariant target pixels for both masks.

The resulting bright and dark target masks contain the CV values for each target i.e. the standardised variation in Brightness across the three dates. This information is used to further classify bright and dark targets according to the probability that they are invariant. Upper and lower thresholds of CV are defined for each of the bright and dark target masks after examination of the frequency histograms.

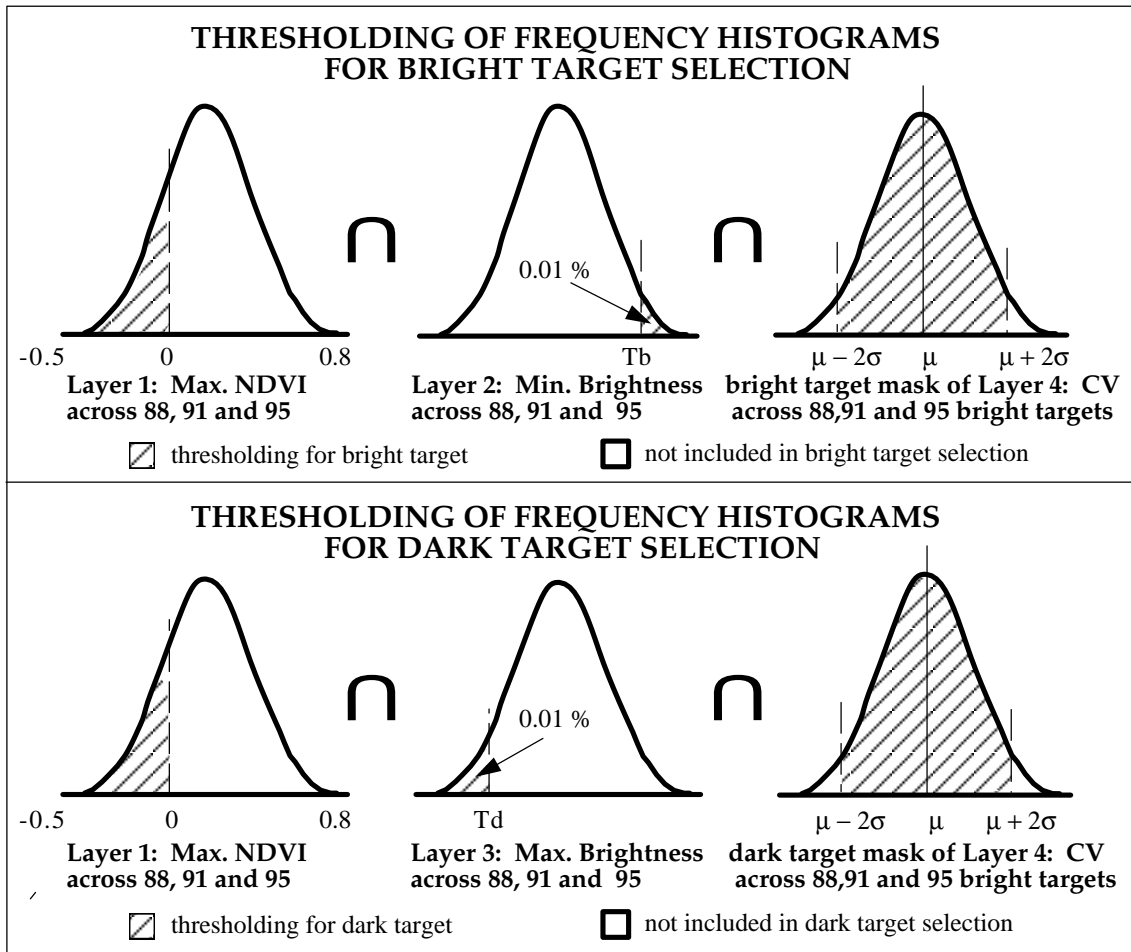


Figure 1. Thresholding the frequency histograms of the four layer composite image to produce masks of bright and dark targets

As it is assumed that the atmosphere has a relatively constant effect over the scene, it is more likely that the invariant targets will be located around the mean of the CV distribution. Experimentation with different ranges of CV has shown that, providing the bright and dark CV histograms are unimodal and continuous about the mean acceptable upper and lower CV thresholds for each mask can be defined on a statistical basis as the mean  $\pm$  two standard deviations. However, additional change factors affecting the targets may result in a bi-modal distribution where a large proportion of pixels on one date are being affected by a given biasing factor, eg. shadowing effects over dark targets (water) or cloud over bright targets. In this case after interpretation, appropriate thresholds are selected to exclude these biased targets, or in the case of cloud on all three dates, the cloud is masked out of the brightness image. In eighty-eight temporal registrations this has been necessary only once.

Before the registration parameters are calculated, the bright and dark target masks are checked to ensure that targets are sensible and that they are well distributed across the scene. Bright targets usually include dry sand, urban features (providing they are not subpixel size) and rocky outcrops on all dates. Dark targets generally include deep, clear water and deep shadows on all dates. In scenes where there are large water bodies (eg. coastal areas), the darkest pixels all tend to occur in one large block (and in some cases, one histogram brightness bin). Large blocks of pixels are generally edited out of the target masks as there is potential for bias resulting from bidirectional reflectance differences from the eastern to the western side of the scene.

Conversely, if there are insufficient targets it is necessary to reiterate the thresholding process. In many cases, especially in western scenes with few deep water bodies, the starting Brightness thresholds based on the frequency histograms are not adequate and thresholding needs to be

reiterated. In the case of one western scene no dark targets could be located at all by varying the greenness and Brightness thresholds. In this case the transformation parameters from an adjacent scene acquired on the same date (and same path) were used.

### Registration Parameters

The invariant target masks are used to compute the set of band means of bright and dark target clusters for each of the three data sets to be registered. The band means are then used to derive the set of transformation parameters.

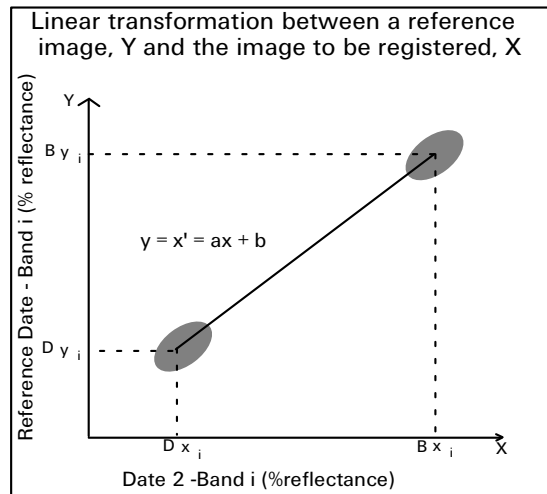


Figure 2. The linear transformation required to equate the invariant targets in band i of two different dates, where  $B_{y_i}$  and  $D_{y_i}$  are the respective bright and dark target means for the reference year and  $B_{x_i}$  and  $D_{x_i}$  are the respective bright and dark target means for the scene to be corrected.

Simple FORTRAN code is used to compute the set of transformation parameters,  $a_i$  and  $b_i$  for every possible registration combination so that an appropriate reference image can be selected. This choice is made on a scene by scene basis. This means that adjacent temporal data sets data may have been registered to a different temporal reference image. The reference image is selected on the basis of atmospheric scattering to enable registration to the clearest possible reference image for any given scene. In using the clearest date, the relative offsets due to atmospheric effects between adjacent scenes are reduced. The image which shows the darkest target means, assumed to have the lowest atmospheric scattering component in TM bands 1, 2 and 3, is taken to be the clearest and is selected as the reference image providing the transformation parameters are reasonable. We assume that we have corrected for nearly all radiometric gain factors in the conversion from digital counts to top of atmosphere reflectance units eg. sensor calibration, sun angle etc. The gains therefore, should be close to 1. If the gains do not reflect this it may be because of 'between-date' spectral variation in the targets. In this case target selection needs to be reassessed. Likewise, the relative offsets should not be consistently high across all bands. The offsets, in these cases, represent the offsets between images due to atmospheric effects. The relative offset can be high for visible bands but should decrease as atmospheric scattering decreases with increasing wavelength.

### Spatial Radiometric Registration

The previous two methods are applied to spatially concurrent data sets. These methods minimise the temporal radiometric differences between scenes acquired in 1988, 1991, and 1995. The methods also aid in the reduction of relative offsets between adjacent scenes by correcting illumination differences and registering to the clearest date. The following methods

complete the radiometric benchmarking of the data by removing any residual radiometric differences between adjacent scenes, not already corrected for in previous stages.

The SLATS solution borrows the common elements from Muller (1993) and Royer *et al.* (1985), by analysing data in overlap areas between adjacent scenes and assuming all data were captured on a common date. Although SLATS data have been purchased over different dates the temporal span has been kept as small as possible. By direct comparison of differences in overlap areas and the removal of these differences using various techniques, SLATS aims to transform its entire image data set to a common radiometric benchmark.

As previously mentioned, for many of the SLATS processing stages it is critical that reference data be relative between adjacent scenes. For all TM data purchased by the SLATS project the scene acquisition dates have been selected to minimise the along-path temporal range. The optimum data set would have been one where along any given path all scenes were captured on the same date. Due to cloud cover this was not possible. The majority of SLATS data however does originate from the same date along any given path. This is critical to the success of the adopted empirical method for resolution of radiometric differences between scenes.

The key assumption that needs to be justified in this method is that data in overlap areas between scenes represents homogeneous ground conditions at any given point in the overlap area. The validity of this assumption for along-path and across-path overlaps will be outlined in the relevant sections that follow.

For this processing stage only scenes captured in 1991 were used in the calculations. The main reason for this being that the 1991 data had the least temporal variance between scene capture dates combined with very low rainfall for the period as compared to either the 1988 or 1995 data sets. All 1991 scenes were captured between mid June and early October. It should be noted that the rainfall for this period of 1991 was extremely low and in fact was the start of a four year El Niño event. A further defining reason for choosing 1991 as the radiometric benchmark year was that 1991 is also the woody vegetation cover mapping benchmark date.

### **Along-path Radiometric Registration**

For along-path radiometric registration any reflectance differences between scenes along a particular path were normalised. This was done by comparing data values which fell exclusively in the overlap area between adjacent north-south scene pairs. East-west anisotropic influences were ignored in this process as the image subtraction of north-south scene pairs effectively eliminates these differences. Any along-path illumination effects were assumed to be corrected by the TM\_REFLECT program. It was theorised that any resultant difference in the mean values of pixels in the common overlap areas would be due to radiometric differences not already corrected for in previous processing stages.

It can be readily accepted that this holds true in the north-south overlap between scenes where the scene pairs were captured on the same day. This is because the reflectance data captured by the sensor should represent exactly the same DN's for both scenes in the overlap area. The acceptance of this assumption becomes more tenuous when the scene pairs are temporally separated by a different overpass epoch.

Any possible changes in ground conditions due to temporal influences will result in differences in DN's that should not be removed as they are real differences and not radiometric errors. To help alleviate this problem, image masks were applied to minimise possible real changes in overlap areas captured at different overpass epochs. Water, crop and topographic shadow effects from either scene were masked out as it was felt that these elements make up the majority of pixels which are likely to be spectrally dynamic over time. Because all 1991 TM data were sourced during the dry season it was theorised that vegetation change would be minimal over such relatively short time intervals. Gross changes in vegetation, such as clearing, were not evident in the north-south overlap areas.

The actual corrections applied to the scenes along a particular path were calculated by first determining the mean difference for each of the six TM bands (1,2,3,4,5 and 7) from the common overlap area between north-south scene pairs. A set of scene corrections for each band are derived so that mean differences in the overlap area between all scene pairs equal

zero. An additional requirement is that no bias is introduced along the path, ie. the sum of the total scene corrections for any given path equal zero.

To gain some idea of the magnitude of the corrections applied the following table of maximum change and mean change has been compiled. The statistics outlined in Table 1 are taken from forty-one scenes in seven paths.

TM BAND	1	2	3	4	5	7
MAXIMUM	12.19	8.49	10.58	6.69	15.56	9.84
MEAN	3.91	1.74	2.78	1.77	4.42	3.35

Table1. Summary of along-path radiometric differences.

### Across-Path Correction

Early in the SLATS project the problem of edge-matching our data was discussed at length. The group was aware of the combined atmospheric and anisotropic influences within individual scenes and across TM paths and was determined to find a solution for what is a major hurdle for any multi-path satellite classification task. Past experience indicated that the western side of any TM satellite scene was generally brighter than the eastern side. The effects of these influences are magnified when the overlap between two adjacent east-west scenes is studied. Across-path radiometric variations make it virtually impossible to classify a full TM scene and get agreement with the neighbouring scene to the east (or west). Prior to across-path correction, FPC classes from the SLATS woody vegetation cover classification were consistently over-estimated in the eastern edges of scenes while under-estimation occurred in the west. The post-correction results from adjacent FPC classifications show a marked improvement in agreement in the east-west overlap areas. Examples of this are depicted in Table 5 and Figure 8 in the Results section.

Solar azimuth relative to the scan line azimuth is also critical. Radiance variations induced by off-nadir viewing are maximal when the scan direction is nearly parallel to the solar azimuth (Royer *et al.*, 1985). In Queensland this is the case for many scenes during summer. Conversely, the effects are minimal when the solar azimuth is orthogonal to the scan line azimuth. This lends further support for the selection of winter image capture dates as the solar azimuth is closer to being normal to the scan line azimuth than summer scenes thus reducing the anisotropic effect.

To minimise across-path radiometric differences a similar methodology to that described in the previous section (along-path radiometric registration) was adopted. No attempt has been made to use analytical techniques, described in the literature, to correct for these differences. Time constraints imposed on the SLATS project dictated the adoption of a rapid empirical solution to the across-path radiometric problem.

Image subtraction in the overlap areas showed fairly consistent differences. Some scene pairs however, demonstrated quite large differences. This was attributed to the fact that the along-path correction had not been applied prior to analysing east-west differences. The east-west differences were therefore re-calculated after the along-path radiometric corrections had been applied. This had the effect of reducing the larger east-west differences. Because the across-path temporal differences were generally greater than the along-path differences some of the results may have been affected by gross change. This was evident in a few cases of trees being cleared in the overlap areas between sensor overpass epochs of east-west scene pairs. While this phenomenon did not occur in the north-south overlaps the probable reasons for it occurring more in the east-west overlaps can be attributed mainly to the larger temporal differences but also because the areas of overlap were far greater for the east-west pairs than for the north-south pairs. Another explanation for the differences can be attributed to the proportion of the object types that form the overlap areas. The mix of non-Lambertian targets (topographic features, trees, and other textured surfaces) relative to the Lambertian-like targets (bare smooth ground, water bodies with no wave structure, and other relatively smooth surfaces) has a marked effect on the overlap area differences (Muller, 1993; Royer *et al.*, 1985).

SLATS decided to adopt the mean of all the east-west differences for its across-path correction values. By adopting this mean correction value for all scenes we accept that the SLATS solution is not the optimal one but the post-correction results support our adoption of this easily applied

rapid technique (see Table 4 in the Results section). A summary of the corrections employed for all scenes is shown in Figure 3 below.

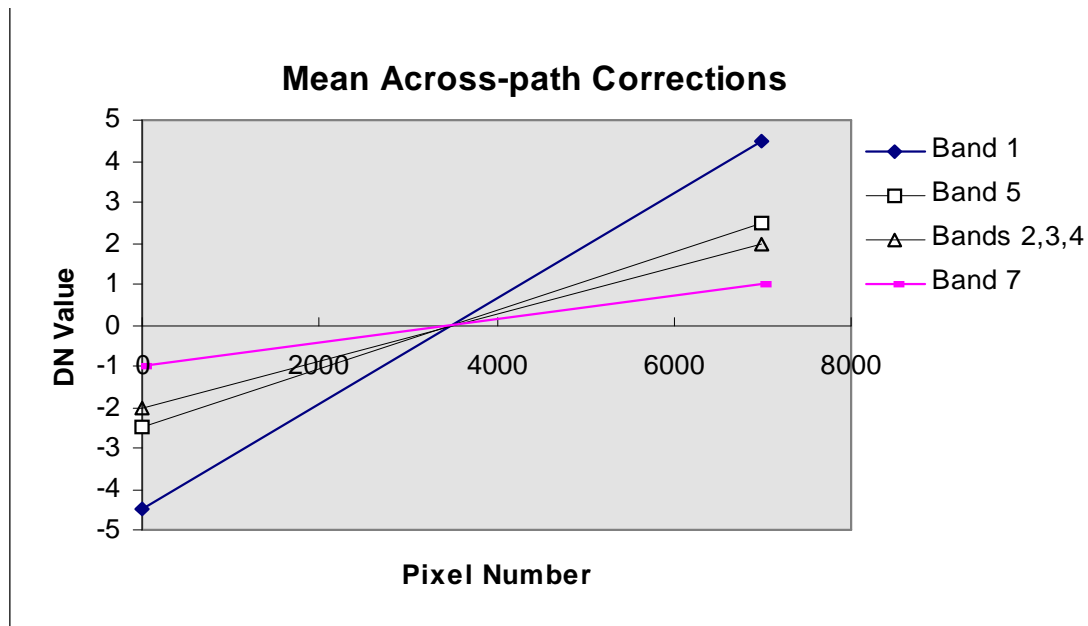


Figure 3. Summary of across-path corrections for combined atmospheric and anisotropic influences applied to all scenes.

While the same measures were taken to limit the effects of real change as were taken with the along-path corrections it is apparent that the east-west differences have been affected more by these changes. The corrections were applied linearly across each band within each scene. Scene centres therefore received no correction while the east and west scene edges gained maximum correction. The final affects of this correction can be seen in the Results section.

## Results

The performance of the correction procedures can only be evaluated in a comparative sense as it is sometimes difficult to separate real change from radiometric mis-registration errors. Where possible, SLATS tried to reduce seasonal effects by selecting the imagery from the dry season of each acquisition year. However, long term seasonal effects are inherent in the imagery. The 1988 and 1991 acquisitions represent the extremes in these conditions. As mentioned previously the 1991 data sets were acquired at the onset of a very dry El Niño event where much of western Queensland was suffering drought conditions. Conversely during the 1988 acquisitions much of Queensland was relatively green.

The results that follow represent:-

- a comparative evaluation of the scene to scene temporal radiometric registration of imagery acquired over Monto for two different dates;
- an evaluation of the spatial radiometric registration affects on wooded/non-wooded discrimination for four scenes (Alpha, Laglan, St Lawrence and Moranbah);
- a comparison of image values in uncorrected versus fully corrected data in the Monto/Bundaberg scene overlap area, testing the combined conversion to TOA reflectance, temporal and spatial procedures ; and
- a comparison between woody FPC classifications prior to and after spatial radiometric registration in the Monto/Bundaberg scene overlap area, testing the results of the SLATS radiometric correction procedure on the final products.

### Scene to scene temporal radiometric transformation applied to imagery acquired over Monto

The two Monto scenes were acquired on 18 July, 1991 and 13 July 1995. The 1991 scene was selected as the reference year as it had consistently lower dark target means across all visible

bands. This was assumed to be the result of lower atmospheric path radiance contributions to visible pixel response. The target cluster means and transformation parameters are listed in Table 2.

<b>TM Band</b>	<b>1</b>	<b>2</b>	<b>3</b>	<b>4</b>	<b>5</b>	<b>7</b>
<b>dark mean 91</b>	45.540	20.355	15.267	15.438	11.244	4.274
<b>bright mean 91</b>	130.819	81.091	117.717	103.021	201.139	104.067
<b>dark mean 95</b>	61.540	27.035	24.653	24.023	24.633	11.291
<b>bright mean 95</b>	138.428	80.812	114.160	101.641	188.061	101.169
<b>slope</b>	1.109	1.129	1.145	1.128	1.162	1.110
<b>offset</b>	-22.718	-10.179	-12.951	-11.669	-17.378	-8.260

Table 2: Slope and offset parameters for temporal radiometric registration of the Monto scene.

A comparative evaluation was conducted using a number of sample data sets not included in bright and dark target selections. The sample sets were extracted from flat, homogeneous cover types which were assumed to be relatively unaffected by seasonal variation and gross change between the two dates. The first sample set includes 5000 pixels extracted from an outcrop of exposed rock from the north-central part of the scene. The second set of data was extracted from numerous areas of homogeneous, dense eucalypt forest. This set included approximately 37,000 pixels with a wide spatial distribution throughout the scene. Band by band comparisons of the sample means for both sample sets are presented in Figure 1. The statistics for the dense forest site are presented in Table 2.

The transformation resulted in a general convergence between reference and transformed data sets. For the exposed rock sample agreement is within 4.8%. Some allowance for non-Lambertian reflectance backscatter off the exposed rock must be made. Results over the vegetation sample are also good with all bands except band 4 showing agreement to within 4.5% between reference and transformed data sets. The band 4 mean offset is actually greater after the transformation by about 6% - increasing from 10.6% to 16.9%. This could be in part due to some radiometric error introduced in the invariant target selection, although this is in conflict with the results over the exposed rock. It is more likely that as band 4 is very sensitive to changes in vegetation dynamics and soil moisture that the bad result is due to seasonal influences on vegetation response.

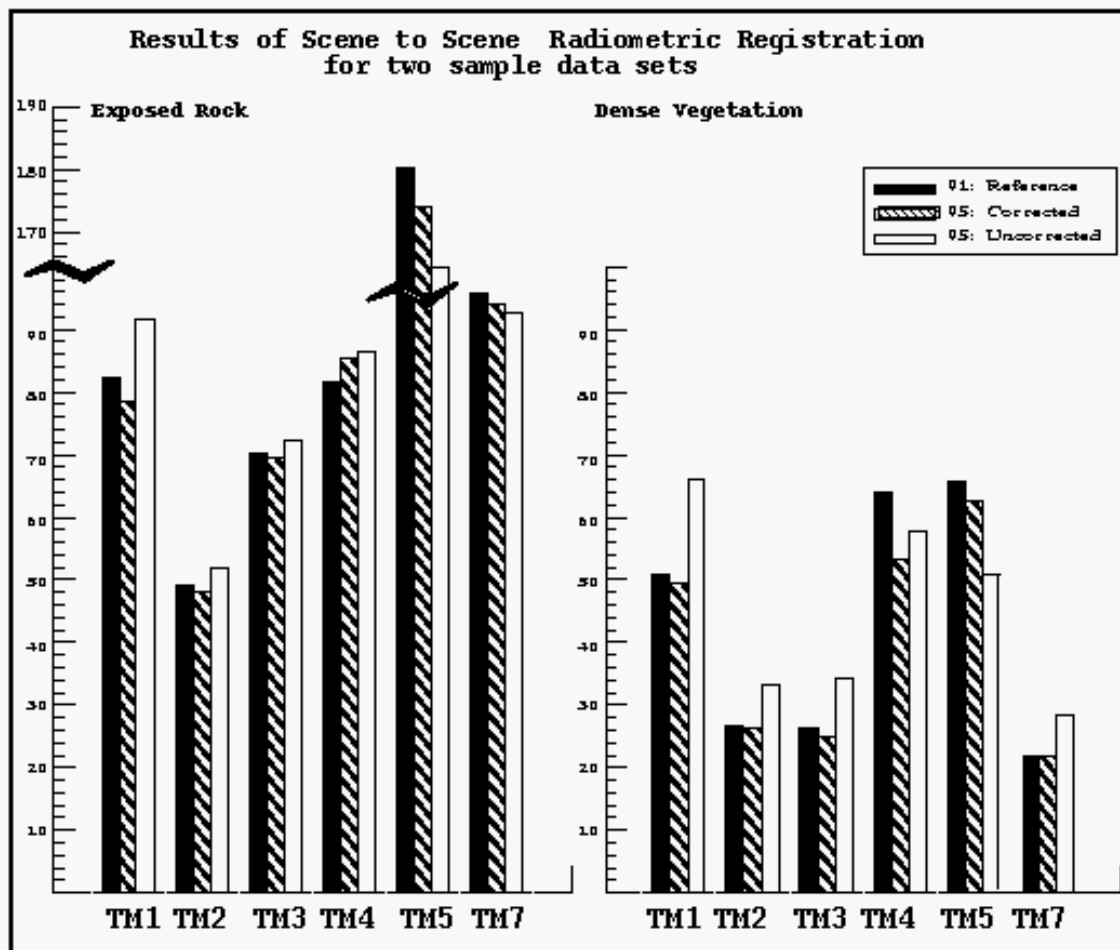


Figure 4: shows the results from the two sample data sets of the transformation

Means of Transformed and Untransformed Data for Sampled Vegetation Pixels						
TM Band	91 TM_REFLECT		95 TM_REFLECT		95 STANDARDISED	
	Mean	St.Dev	Mean	St.Dev	Mean	St.Dev
Band 1	50.82	3.18	66.17	4.14	49.39	5.00
Band 2	50.82	3.18	66.17	4.14	49.39	5.00
Band 3	26.29	2.67	34.27	3.16	25.09	4.00
Band 4	64.09	7.43	57.86	4.75	53.31	5.33
Band 5	65.82	8.63	50.74	7.84	62.73	9.96
Band 7	21.94	4.20	28.27	4.45	21.82	5.35

Table 3: Comparison of band by band means for transformed and untransformed data. Evaluation was conducted on a sample of 37,000 pixels of dense vegetation spatially distributed evenly throughout the Monto scene.

**Spatial radiometric registration affects on wooded/non-wooded discrimination for four scenes.**

Four typical scenes have been selected from the SLATS image data set to demonstrate the affects of spatial radiometric registration affects on wooded/non-wooded discrimination. Alpha,

Laglan and Moranbah are from the central Queensland region while St Lawrence is an adjacent coastal scene. Data for all four scenes were captured in 1991. A method of feature space classification using TM band 5 and NDVI is used by SLATS to discriminate wooded from non-wooded vegetation (Kuhnell *et al.*, 1998). Initial comparison of wooded/non-wooded discrimination lines for these scenes indicated significant radiometric differences existed (see Figure 5). The data being compared had previously been converted to top of atmosphere reflectance values and in some cases registered to another date image during the temporal radiometric registration stage. Concern was expressed at the large separation between the curves, especially at the A-B separation position in feature space. This area of feature space represents high data frequencies within the scenes concerned. Any difference between the curves in this area therefore represents large discrepancies in the final classifications. Early comparison of the wooded/non-wooded classifications in the overlap areas between scenes verified these discrepancies.

### NDVI and TM Band 5 Feature Space

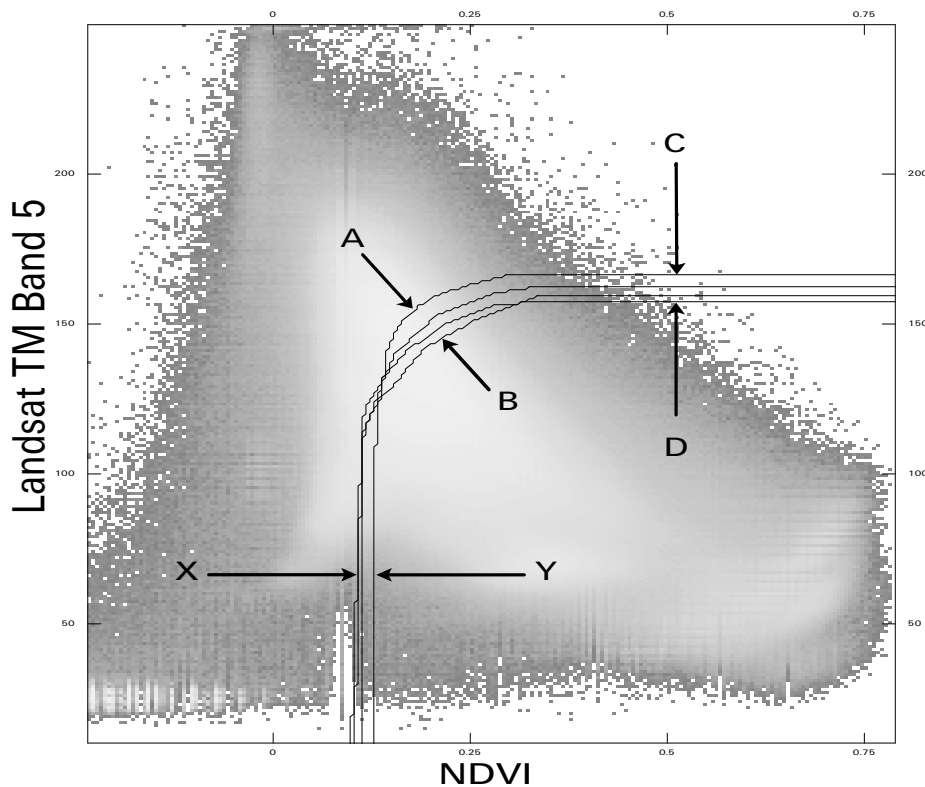


Figure 5: Wooded/non-wooded delineations for Alpha, Laglan, St Lawrence and Moranbah prior to spatial radiometric correction.

After the spatial radiometric registration process had been completed for the four scenes the same user defined curves were re-calculated using feature space values derived from the corrected scene values. These new curves can be seen in Figure 6. The key difference is the reduction in separation between the curves at A-B. This is a direct result of the spatial radiometric registration process as no new operator interpretation of the wooded/non-wooded delineations were conducted. Qualitative comparison between Figure 5 and Figure 6 show improvement in the convergence of the curves at A-B and C-D but little convergence at X-Y. A suggested reason for this is that the NDVI is a ratio of bands and therefore the band corrections have little effect on NDVI.

## NDVI and TM Band 5 Feature Space

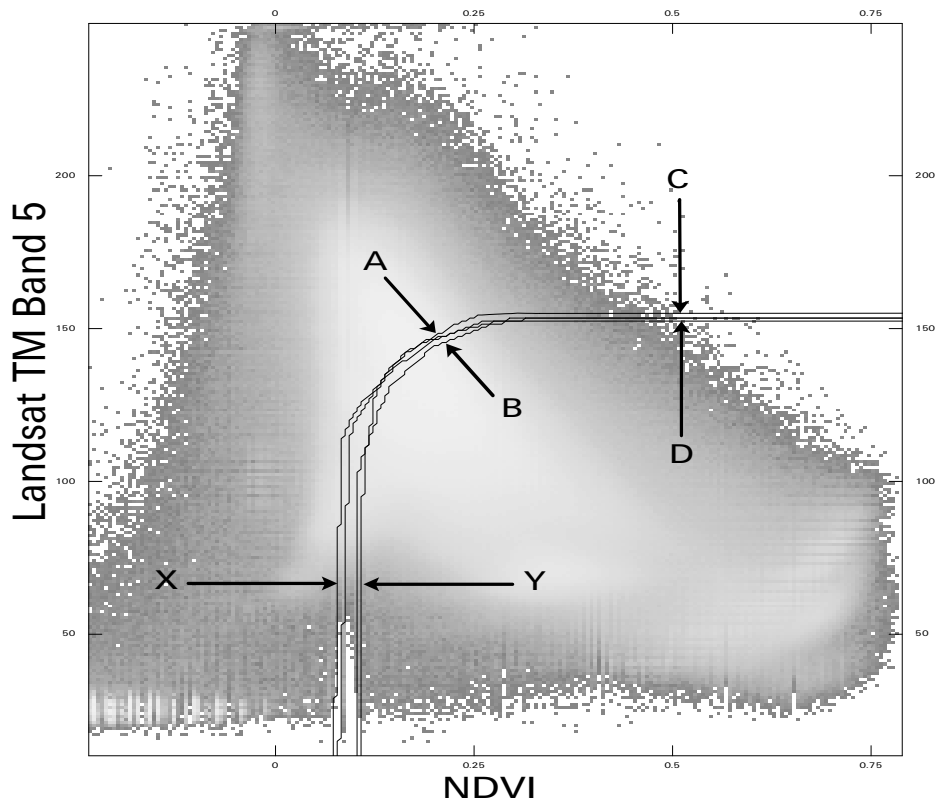


Figure 6: Wooded/non-wooded delineations for Alpha, Laglan, St Lawrence and Moranbah after spatial radiometric correction.

### Comparison of image values in uncorrected versus fully corrected data in the Monto/Bundaberg scene overlap area.

To gauge the magnitude of the combined radiometric corrections applied to the SLATS image data a quantitative comparison of uncorrected versus fully corrected data is presented. The uncorrected data represent Level 5 processed data values as received from ACRES for the Bundaberg scene (captured 29<sup>th</sup> September 1991) and the Monto scene (captured 18<sup>th</sup> July 1991). The fully corrected data has had the conversion to top of atmosphere reflectance, temporal radiometric registration and spatial radiometric registration processing applied to it.

The sample data set represented 80, 000 pixels extracted from the overlap area. The sample statistics summarised in Table 4 show marked convergence between the means in all bands. An alternative graphical presentation of these results is shown in Figure 7. Perfect registration is not expected as the spatial radiometric process uses mean corrections for along-path and across-path differences.

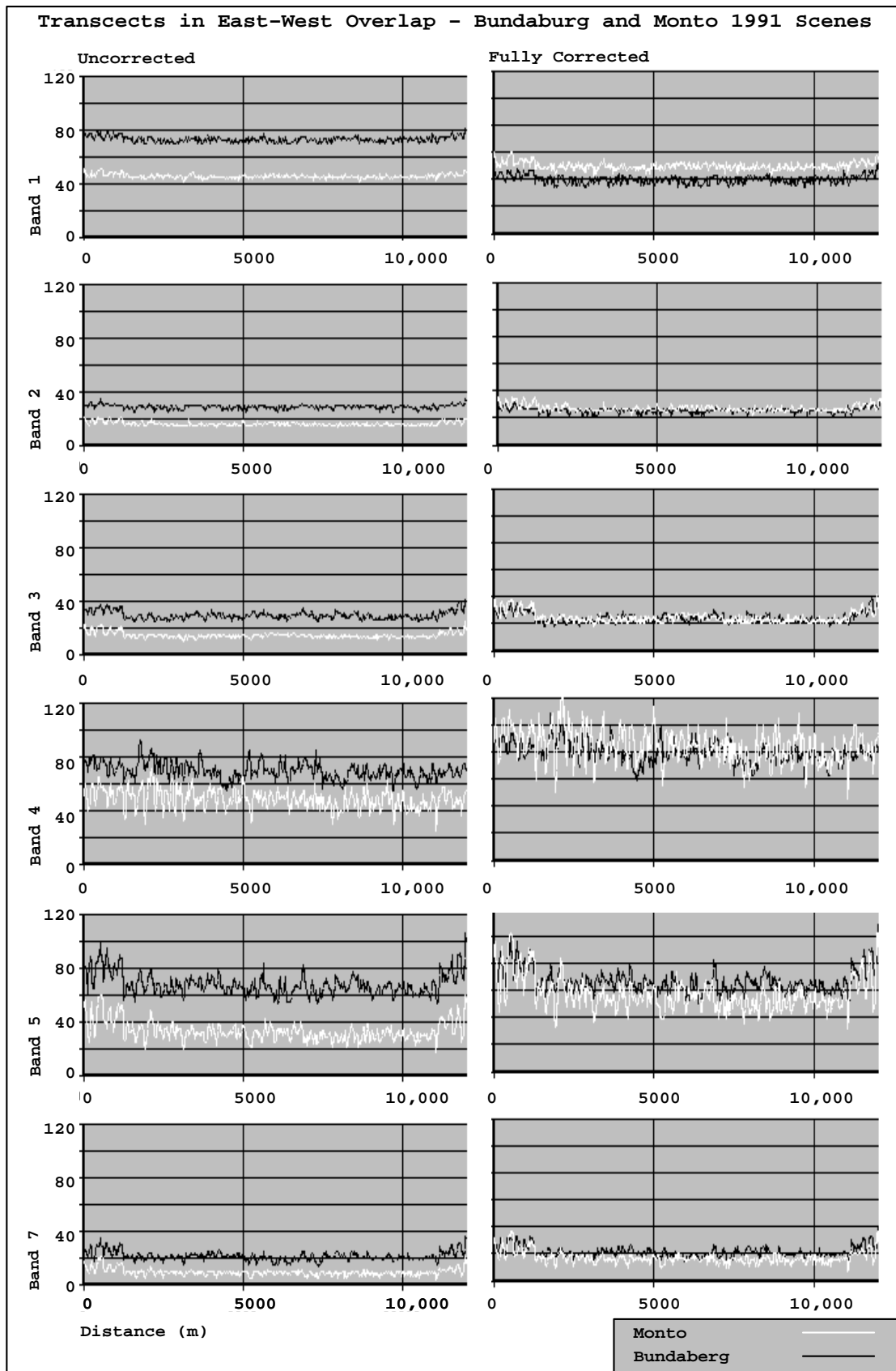


Figure 7: Uncorrected data transects versus fully corrected data transects in the Bundaburg/Monto overlap area.

<b>TM Band</b>	<b>Uncorrected 1991 Data</b>				<b>Fully Corrected 1991 Data</b>			
	Bundaberg		Monto		Bundaberg		Monto	
	<b>Mean</b>	<b>St.Dev.</b>	<b>Mean</b>	<b>St.Dev.</b>	<b>Mean</b>	<b>St.Dev.</b>	<b>Mean</b>	<b>St.Dev.</b>
<b>Band 1</b>	78.87	4.06	46.84	1.75	48.32	5.70	53.38	3.39
<b>Band 2</b>	31.35	2.17	16.91	1.30	29.91	3.33	29.05	2.34
<b>Band 3</b>	36.35	4.81	16.39	2.17	34.02	6.39	28.50	3.67
<b>Band 4</b>	64.07	5.93	40.14	7.20	72.85	7.32	71.88	11.72
<b>Band 5</b>	82.97	12.06	37.62	6.62	83.61	13.27	66.43	11.37
<b>Band 7</b>	30.11	7.07	11.96	3.17	32.08	8.28	22.35	5.51

Table 4: Summary of uncorrected versus fully corrected data values taken from the overlap area between the Bundaberg and Monto scenes.

**Woody FPC classifications prior to and after spatial radiometric registration in the Monto/Bundaberg scene overlap area.**

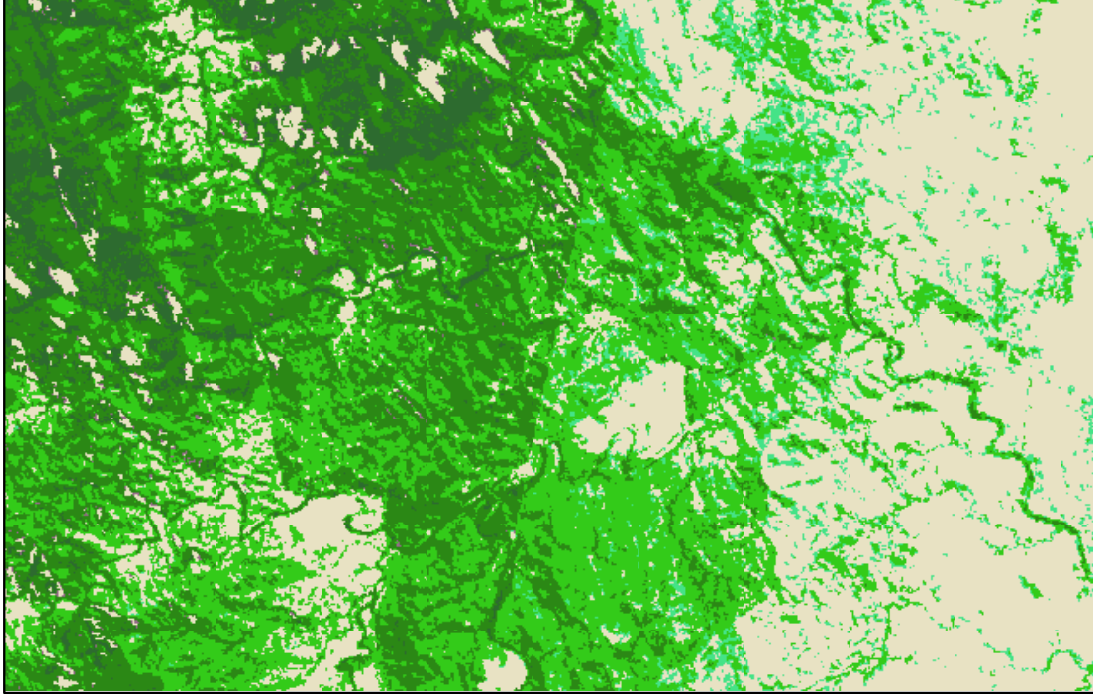
The improvements noted in the SLATS cover classification due to the spatial radiometric registration are dramatic. Table 5 quantitatively shows the convergence between the mean FPC values post spatial registration as opposed to the pre-spatial registration means. A qualitative appraisal of the effects of spatial radiometric registration can be gleaned from Figure 8 which shows the SLATS woody FPC classification outputs prior to and post registration. The edge join between the mosaiced scenes can easily be seen in the uncorrected image (top) where no such edge effect is apparent in the spatially radiometrically registered scenes (bottom).

	<b>POST REGISTRATION</b>		<b>PRE - REGISTRATION</b>	
	<b>BUND</b>	<b>MONT</b>	<b>BUND</b>	<b>MONT</b>
<b>Mean (%FPC)</b>	42.2005	42.4317	39.5353	46.8554
<b>St. Dev</b>	17.7894	14.3004	17.4058	16.7349

Table 5: Foliage Projective Cover mean values from transects in the Bundaberg/Monto overlap area prior to and post spatial radiometric registration.

## Two Scene Mosaic of Woody %FPC Classification - Bundaberg and Monto Scenes

**Before East-West Correction**



**After East-West Correction**

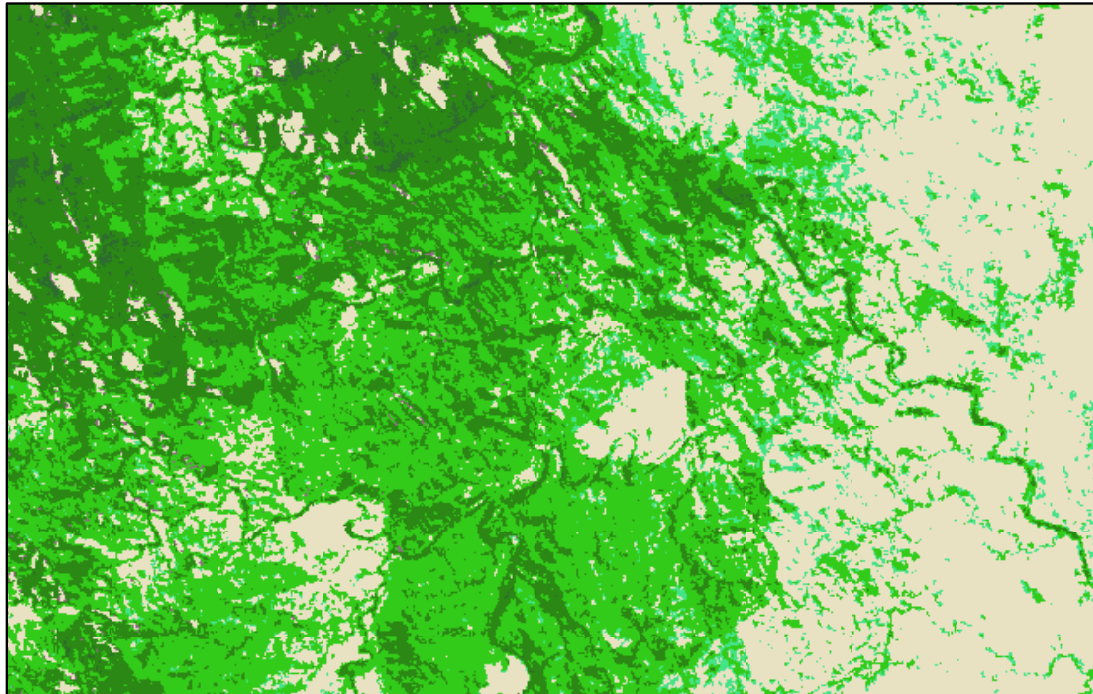


Figure 8: Woody FPC classifications over the Bundaberg/Monto scene area prior to and post spatial radiometric classification.

## Conclusions

At the time of publishing, SLATS has successfully completed the temporal radiometric registration of the complete set of 1987/88, 1990/91 and 1994/95 data sets (88 scene temporal data sets comprising 176 registrations in total) and has commenced registering the 1997 data to these sets. Spatial radiometric registrations have been completed for seven of the twelve paths of imagery covering Queensland (41 scenes).

Successful results from the radiometric registration procedures have significantly contributed to the quality and development of baseline landcover and woody vegetation cover maps and the final mosaiced products. In addition, the corrections applied have improved the ability to correctly classify the 88 TM scenes that cover Queensland. Time saved in edgematching the data has been enormous although difficult to quantify.

The radiometric registration methodologies presented here have resulted in the overall radiometric benchmarking of the entire dataset to a best-fit approximation. While not all the radiometric differences have been removed the radiometric corrections applied have allowed relative comparisons between temporal and spatial data sets. The methods could undoubtedly be improved with a more thorough investigation of sensor calibration, anisotropic and atmospheric effects but operational requirements of the project have limited this capability. The resources required to achieve a minor data quality credit is not justifiable for the SLATS project at this time.

## Acknowledgements

The authors would like to thank: the Queensland Government for their vision and support of this work, especially a \$7.2 million Special Treasury Initiative grant without which all of this would not be possible; the DNR Resource Management and Resource Sciences and Knowledge directorate; all the DNR Climate Impacts and Grazing Systems staff and DPI Tropical Beef Centre staff who have contributed to the development and testing of this work; the project advisory committee for their advice and enduring support of the project; and the Commonwealth Bureau of Resource Sciences which contributed 10% of the projects first-term funding.

## References

- Chavez, P.S. Jnr, 1989. Radiometric calibration of Landsat Thematic Mapper multispectral images. *Photogrammetric Engineering and Remote Sensing*, 55:1285-1294.
- Crippen, R. E. 1987. The Regression Intersection Method of adjusting image data for band rationing. *International Journal of Remote Sensing*, 8(2):137-155
- Danaher, T.J., G. Bisshop, L. Kastanis, and J. Carter, 1998. The Statewide Landcover and Trees Study (SLATS) - monitoring landcover change and greenhouse gas emissions in Queensland. *Proceedings of the 9<sup>th</sup> Australasian Remote Sensing and Photogrammetry Conference*, Sydney, Australia, July 1998.
- Hall, F.G., D.E.Strebel, J.E.Nickeson, and S.J.Goetz, 1991. Radiometric rectification: towards a common radiometric response among multitemporal, multisensor images. *Remote Sensing of Environment*, 35:11-27.
- Herman, B. M., and S. R. Browning, 1975. The effect of aerosols on the earth-atmosphere albedo. *Journal of Atmospheric Science*, 32:158-165
- Holm, R.G., R.D. Jackson, and B. Yuan, 1989. Surface reflectance factor retrieval from Thematic Mapper data. *Remote Sensing of Environment*, 27:47-57.
- Kuhnell, C., B. M. Goulevitch, T.J. Danaher, D. P. Harris, 1998. Mapping Woody Vegetation Cover Over Queensland using Landsat TM Imagery. *Proceedings of the 9<sup>th</sup> Australasian Remote Sensing and Photogrammetry Conference*.

- Moran, M. S., R. D. Jackson, G. F. Hart, 1990. Obtaining surface reflectance factors from atmospheric and view angle corrected SPOT-1 HRV data. *Remote Sensing of Environment*, 32:203-214.
- Moran, M. S., R. D. Jackson, P.N. Slater, and P.M. Teillet, 1992. Evaluation of simplified procedures for retrieval of land surface reflectance factors from satellite sensor output. *Remote Sensing of Environment*, 41:169-184
- Muller, E., 1993. Evaluation and correction of angular anisotropic effects in multirate SPOT and Thematic Mapper data. *Remote Sensing of Environment*, 45:295-309.
- Paltridge, G. W., and R. M. Mitchell, 1990. Atmospheric and viewing angle correction of vegetation indices and grassland fuel moisture content derived from NOAA/AVHRR. *Remote Sensing of Environment*, 31:121-135.
- Royer, A., P. Vincent, and F. Bonn, 1985. Evaluation and correction of viewing angle effects on satellite measurements of bidirectional reflectance. *Photogrammetric Engineering and Remote Sensing*, 51:1899-1914.
- Schott, J. R., C.Salvaggio, and W.J. Volchok, 1988. Radiometric scene normalisation using pseudoinvariant features, *Remote Sensing of Environment*, 26:1-16.
- Slater, P.N., S.F. Biggar, R.G. Holm, R.D. Jackson, Y. Mao, M.S. Moran, J.M. Palmer, and B. Yuan, 1987. Reflectance- and radiance-based methods for the in-flight absolute calibration of multispectral sensors, *Remote Sensing of Environment*, 22:11-37
- Switzer, P., W. S. Kowalik, and R. J.P Lyon, 1981. Estimation of Atmospheric Path Radiance by the Covariance Matrix Method. *Photogrammetric Engineering and Remote Sensing* 47(10).
- Vanouplines, P.I.G.M., 1986. A simple atmospheric correction algorithm for Landsat Thematic Mapper satellite images, *Symposium on Remote Sensing for Resources Development and Environmental Management*, Enschede, August 1986
- Vermote, E., D. Tanré, J. L. Deuzé, M. Herman, and J.J. Morcrette, 1994 *Second Simulation of the Satellite Signal in the Solar Spectrum (6S)*
- Walls, J., L. Kastanis and J. Plunkett, 1998. Development of integrated products for tree management planning. *Proceedings of the 9<sup>th</sup> Australasian Remote Sensing and Photogrammetry Conference*, Sydney, Australia, July 1998
- Whitlock, H., S. R. LeCroy, and R. J. Wheeler, 1994. Narrowband angular reflectance properties of the alkali flats at White Sands, New Mexico. *Remote Sensing of Environment*, 50:171-181.